Thermochimica Acta, 33 (1979) 69—86

DSC STUDY OF MELTING AND SOLIDIFICATION OF SALT HYDRATES

STANLEY CANTOR

Chemistry Division, Oak Ridge National Laboratory, P.O. Box X, Oak Ridge, TN 37830 (U.S.A.)

(Received 30 October 1978)

ABSTRACT

Most salt hydrates, especially those proposed for thermal-energy-storage applications, melt incongruently. In static systems, this property often leads to differences between the enthalpy of fusion and enthalpy of solidification. By means of differential scanning calorimetry (DSC), these differences have been determined for several salt hydrates. For $Na_2SO_4 \cdot 10\ H_2O$, the enthalpy of solidification at or near the peritectic temperature is never more than 60% of the enthalpy of fusion; further cooling leads to a second phase transition at a temperature corresponding to eutectic melting of mixtures of ice and this hydrate. This asymmetrical melting and freezing behavior of $Na_2SO_4 \cdot 10\ H_2O$ decreases its potential as an energy-storing medium and also limits its usefulness for temperature calibration of DSC instruments. Sodium pyrophosphate decahydrate, $Na_4P_2O_7 \cdot 10\ H_2O$, although in some ways a higher temperature analog of $Na_2SO_4 \cdot 10\ H_2O$, exhibited a smaller discrepancy between the enthalpies of fusion and of solidification; its relatively high transition temperature permits a more rapid solidification reaction than is the case for $Na_2SO_4 \cdot 10\ H_2O$. For $Mg(NO_3)_2 \cdot 6\ H_2O$, a congruently melting compound, the magnitude of ΔH of crystallization equalled ΔH of fusion, even when supercooling occurred; a solid-state transition at 73°C, with $\Delta H = 2.9$ cal g^{-1}, was detected for this hydrate. $MgCl_2 \cdot 6\ H_2O$, which melts almost congruently, exhibited no disparity between ΔH of crystallization and ΔH of fusion. $CuSO_4 \cdot 5\ H_2O$ and $Na_2B_4O_7 \cdot 10\ H_2O$ exhibited marked disparities. $Na_2B_4O_7 \cdot 10\ H_2O$ formed metastable $Na_2B_4O_7 \cdot 5\ H_2O$ at the phase transition; this was derived from the transition temperature and verified by relating the observed ΔH of transition to heats of hydration. Peritectic solidification of hydrates can be viewed as a dual process: crystallization from the liquid solution and reaction of the lower hydrate (or anhydrate) with the solution; where ΔH of solidification appears to be less in magnitude than the ΔH of fusion, the difference can be attributed to slower reaction rate between solution and the lower hydrate. New or previously unreported values for ΔH of fusion obtained in this study were, in cal g^{-1}: $Mg(NO_3)_2 \cdot 6\ H_2O$, 36; $Na_4P_2O_7 \cdot 10\ H_2O$, 59; $CuSO_4 \cdot 5\ H_2O$, 32; $Na_2B_4O_7 \cdot 10\ H_2O$, 33.

INTRODUCTION

The general purpose of this study was to gain a greater understanding of the melting and freezing behavior of inorganic salt hydrates. These compounds are potentially valuable media for isothermal heat storage in residential and commercial buildings. Most salt hydrates melt incongruently; this property appears to affect the amount of energy that can be reliably retrieved from storage. Thus, this investigation was concerned with uncovering any disparity between the enthalpy of fusion (heat stored) and the

enthalpy of solidification (heat retrieved) at or near the peritectic temperature of salt hydrates.

When an incongruently melting salt hydrate, denoted $S \cdot xW$, is heated to its (peritectic) melting temperature, T_m, two new phases appear: a hydrate with y waters per mole of salt and a liquid phase with z waters per mole of dissolved salt, such that $y < x < z$. At T_m, the liquid phase (the peritectic solution) is in equilibrium with two solid phases and the phase equilibrium can be written as

$$S \cdot xW = \left[1 - \frac{(x-y)}{(z-y)}\right] S \cdot yW + \left[\frac{(x-y)}{(z-y)}\right] S \cdot zW \text{ (soln)} \quad (1)$$

The bracketed terms are equal to mole fractions of reaction products provided 1 mole of $S \cdot xW$ is melted. Reaction (1) is, in essence, a disproportionation reaction in which the waters of hydration in the original hydrate, $S \cdot xW$, disproportionate into (a) a liquid with a higher mole ratio (z) of water to salt, and (b) another solid with a lower mole ratio (y). In the melting of some hydrates (e.g., $Na_2SO_4 \cdot 10\ H_2O$) y is zero; the solid reaction product is, therefore, an anhydrate. At temperatures above the peritectic, $T_m + \delta T$, the original hydrate $S \cdot xW$ disappears; reaction (1) has proceeded completely to the right and equilibrium at constant temperature and pressure is defined by two phases only, $S \cdot zW$ (soln.) and $S \cdot yW$.

It is a commonplace experience that the initial melting of an incongruently melting hydrate occurs quite readily. When the products of reaction (1) cool, processes other than the reverse of (1) often occur: $S \cdot xW$ appears to crystallize only from the solution phase (which may also have supercooled); $S \cdot yW$ reacts very slowly as if impeded by some barrier to reaction with the solution. In this study, the nature of the barriers preventing equilibrium solidification were not directly investigated. Instead, by combining DSC results with information contained in phase diagrams, mechanisms of solidification were inferred.

Differential scanning calorimetry has been shown to be a very useful means for examining phase behavior in thermal storage media [1]. In an earlier, brief investigation, the author [1] showed that for $Na_2SO_4 \cdot 10\ H_2O$ (often referred to as Glauber's salt) the enthalpy of solidification was considerably less than the enthalpy of fusion initially measured; in this investigation, a more thoroughgoing set of DSC measurements were run to gain a greater insight into the phase transition behavior of this important energy-storage material. To contrast the behavior of Glauber's salt, five other salt hydrates were studied by DSC methods as part of the investigation; four of these compounds melt incongruently; the fifth, $Mg(NO_3)_2 \cdot 6\ H_2O$, melts congruently and was studied to be more certain that discrepancies (observed for incongruently melting hydrates) in ΔH of fusion and ΔH of solidification were not an artifact of the calorimeter. For the hydrates studied, the phase equilibrium reactions [eqn. (1)] were calculated from critically evaluated solubility data [2]. The reactions are given in Table 1.

The earlier study [1] showed that DSC exothermic measurements tend to amplify supercooling tendencies; the greater supercooling may be associated with the small sample size in the shallow-pan configuration. Therefore, for

TABLE 1

Solid—liquid phase transition of several inorganic salt hydrates

Hydrate	Melting point (°C)	Type of melting	Equilibrium reaction (see eqn. (1))	Ref. 2
$Na_2SO_4 \cdot 10\ H_2O$	32.4	Incongruent	$S \cdot 10W \rightleftharpoons 0.3695\ S + 0.6305\ S \cdot 15.86W$ (soln)	Vol. II, p. 1122
$Na_4P_2O_7 \cdot 10\ H_2O$	79.5	Incongruent	$S \cdot 10W \rightleftharpoons 0.612\ S + 0.388\ S \cdot 25.8W$ (soln)	Vol. II, p. 1106
$Mg(NO_3)_2 \cdot 6\ H_2O$	89.5	Congruent	$S \cdot 6W \rightleftharpoons S \cdot 6W$ (soln)	Vol. II, p. 511
$MgCl_2 \cdot 6\ H_2O$	116.7	Incongruent	$S \cdot 6W \rightleftharpoons 0.070\ S \cdot 4W + 0.930\ S \cdot 6.15W$ (soln)	Vol. II, p. 480
$CuSO_4 \cdot 5\ H_2O$	95.6	Incongruent	$S \cdot 5W \rightleftharpoons 0.766\ S \cdot 3W + 0.234\ S \cdot 11.56W$ (soln)	Vol. I, p. 966
$Na_2B_4O_7 \cdot 10\ H_2O$	58.5	Incongruent	$S \cdot 10W \rightleftharpoons 0.903\ S \cdot 4W + 0.097\ S \cdot 65.8W$ (soln)	Vol. II, p. 820
	60.8	Incongruent, Metastable	$S \cdot 10W \rightleftharpoons 0.902\ S \cdot 5W + 0.098\ S \cdot 55.9W$ (soln)	

each hydrate, other than Glauber's salt, supercooling was also measured by conventional cooling-curve methods in test tubes containing samples weighing 10—40 g.

EXPERIMENTAL

All DSC measurements were carried out with a Perkin-Elmer Model DSC-2. Most data were integrated from the recorded output by means of the electronic planimeter previously described [1]. For transitions with equal baseline heights before and after the transition, the data were integrated as they were being recorded by means of a voltage-to-frequency converter unit similar to that used in integrating chromatographic peaks; built into this unit is a "buffer" amplifier, an integrated circuit, that permits the DSC signal to be read simultaneously by the recorder and the unit. With this device the number of counts appearing on its optical display is proportional to the area under the curve. The baseline on the integrator is fine-tuned by observing the baseline being drawn on the recorder and adjusting the potentiometer on the device.

The instrument was calibrated and tested with two materials: high purity indium metal and distilled water. In the case of indium, a large number of alternating endothermic and exothermic scans at rates of 1.25 and 2.5°C min^{-1} generally showed that heat evolved on freezing equalled heat absorbed on melting; although most exotherms revealed some supercooling, this was seldom more than 3°C. With water, the results were somewhat different. Extensive supercooling (20—23°C) could not be avoided without using AgI as a nucleating agent; without nucleation and at a sensitive attenuator setting ("Range" = 0.2 mcal sec^{-1}), the apparent enthalpy of freezing could be as much as 25% less than the enthalpy of melting. With nucleation, the enthalpy observed on freezing was equal to the enthalpy of melting. All endotherms, with or without AgI, yielded the expected ΔH of fusion for ice within about 5%; these results were obtained whether or not the previous exotherm showed a deficient enthalpy of freezing. These DSC experiments on the ice—water transition indicated that the instrument's differential power circuit could be saturated by the exothermic change; however, it was also clear that a prompt endothermic scan could resolve this question of instrument performance.

All samples, including indium and water calibration samples, were sealed in aluminum volatile sample pans. Samples were weighed with a Mettler Model ME 22 microbalance. Since hydrates either volatilize or absorb moisture when exposed to laboratory air (borax is an exception), samples were loaded and sealed quickly. Weight gains or losses were kept to less than 5 μg, or less than 0.1% of the usual sample size.

In general, analytical-reagent or reagent-grade chemicals were used in sample preparation. The $Na_2SO_4 \cdot 10\ H_2O$ (Fisher "Certified", Fischer Scientific Co., Fair Lawn, N.J.) was found to contain 43.4 wt.% Na_2SO_4 (theoretical for the decahydrate, 44.08 wt.%); the analysis was carried out in platinum containers by first heating in a 125°C oven over a weekend; samples for

analysis were subsequently heated for about 2 h in a 850°C muffle furnace (experience showed that additional weight losses at 850°C were negligible); thus, the source material possessed the equivalent formula $Na_2SO_4 \cdot 10.28\ H_2O$, the slight hyperstoichiometry also detected by the DSC from the presence of the ice— $Na_2SO_4 \cdot 10\ H_2O$ eutectic at —1.1°C (see below). Three types of samples were prepared for study: (i) $Na_2SO_4 \cdot 10\ H_2O$ alone; (ii) $Na_2SO_4 \cdot 10\ H_2O$ with borax, 2—9 wt.%; (iii) $Na_2SO_4 \cdot 10\ H_2O$ with borax (~4 wt.%) and anhydrous Na_2SO_4 (also Fisher "Certified" grade).

For $Mg(NO_3)_2 \cdot 6\ H_2O$ and $MgCl_2 \cdot 6\ H_2O$, analytical reagent (Mallinckrodt Chemical Co.; St. Louis, Mo) material was used without further treatment. Karl Fischer titration yielded: 42.1% H_2O for $Mg(NO_3)_2 \cdot 6\ H_2O$ (calc. 42.16%); 54.2% H_2O for $Mg(NO_3)_2 \cdot 6\ H_2O$ (calc., 53.17%); the composition of the magnesium chloride hexahydrate, therefore, corresponds to $MgCl_2 \cdot 6.25\ H_2O$.

Fischer "Certified" $Na_4P_2O_7 \cdot 10\ H_2O$ and $CuSO_4 \cdot 5\ H_2O$ were used as received. The decahydrate consisted of fairly large (1—8 mm) crystalline fragments; smaller crystals were selected for DSC samples; analysis for water by Karl Fischer reagent yielded 40.4%, calc. for $Na_4P_2O_7 \cdot 10\ H_2O$, 40.39%. Water analysis for copper sulfate pentahydrate yielded 33.5%, calc., 36.08%; the analysis corresponds to the formula, $CuSO_4 \cdot 4.5\ H_2O$.

Reagent-grade $Na_2B_4O_7 \cdot 10\ H_2O$ (B&A Specialty Chemicals Division, Allied Chemical Co., Morristown, N.J.) was used without further treatment. Since Karl Fischer titrations gave inconsistent H_2O analyses, samples were checked for excess water in the DSC by first cooling to —40°C and then seeking to detect the ice—borax eutectic at —0.43°C [3]; this transition was not detected.

For determining supercooling in samples 10—40 g in weight, the hydrates were loaded into large test tubes, each fitted with a metal-sheathed chromel—alumel thermocouple passing through a rubber stopper. The thermocouple was connected to a digital temperature indicator, Doric Model DS-350. Samples were melted by partially immersing the test tube in an oil bath set 10—15° above the melting point; the sample was then cooled at about 0.5° min^{-1} by reducing power to the bath. The onset of crystallization was observed by noting temperatures on the digital indicator; for $MgCl_2 \cdot 6\ H_2O$, the onset of crystallization could also be observed visually.

RESULTS AND DISCUSSION

$Na_2SO_4 \cdot 10\ H_2O$

The enthalpy of fusion obtained on first heating samples of $Na_2SO_4 \cdot 10\ H_2O$ was 57.7 cal g^{-1}, this value corrected for the additional H_2O, 1.5 wt.% determined by analysis. The small negative discrepancy from the more accurate literature [4] value (58.57 ± 0.06 cal g^{-1}) is associated with the effect of the (water) impurity that forms a eutectic.

Figure 1 presents the thermal spectra generated when $Na_2SO_4 \cdot 10\ H_2O$ is initially heated through two thermal cycles, the data for both cycles having

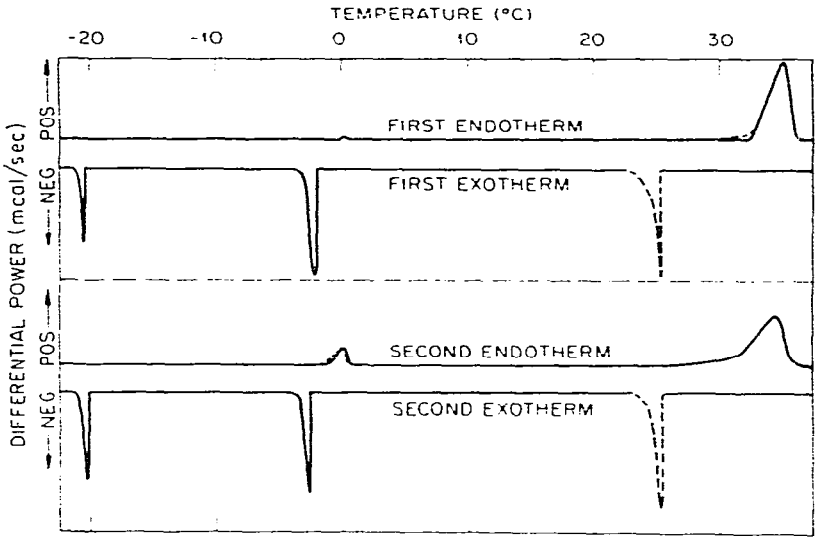

Fig. 1. Typical DSC thermal spectra obtained for $Na_2SO_4 \cdot 10\ H_2O$ (solid lines). Dotted lines show changes that occur when $Na_2B_4O_7 \cdot 10\ H_2O$ (2—9 wt.%) is added to the sample.

been obtained within 24 h. After first cooling the sample to —20°C, the initial endotherm showed a barely perceptible transition just below 0°C; this is attributed to the eutectic melting of ice and $Na_2SO_4 \cdot 10\ H_2O$ [3]; the enthalpy of transition was quite small, equivalent to less than 0.1 mcal mg^{-1} of sample. The sharp peak of the first endotherm is due to (peritectic) melting that begins at about 32°C. The exotherm obtained soon after the initial melting (labelled "First Exotherm" in Fig. 1) shows two spiked peaks at —2 and —20°C with shapes characteristic of crystallization from supercooled liquids; the nearly vertical deflection signifies the rapid release of energy caused by the sudden onset of crystallization. The area of the peak at —2°C was equivalent to 30 cal g^{-1}, slightly more than half of the enthalpy of fusion obtained from the first endotherm. At —20°C, a second phase transition occurs; this is attributed to the (supercooled) eutectic at which water and dissolved $Na_2SO_4 \cdot 10\ H_2O$ crystallize; solidification is now complete. The area of this peak, equivalent to 10—15 cal g^{-1}, was always less than the area of the peak at —2°C.

The next heating of the sample ("Second Endotherm", Fig. 1) showed a well-defined transition near 0°C; from the intersection of the leading edge and the baseline, we obtain —1.1°C, in agreement with the value [3] for the melting point of the eutectic mixture of ice and $Na_2SO_4 \cdot 10\ H_2O$. The next transition, peaking at 35°C, signified that the sample had remelted. The positive slope in the baseline beginning at about 20°C is . further indication that an "impurity", not present in the initial endotherm, had grown into the sample. The sloping baseline led to greater uncertainty in calculating the enthalpy of fusion than was the case for the first endotherm; but, even including the interval 20 to 32°C in integrating the area, the ΔH of fusion was about 30 cal g^{-1} for endothermic scans taken within a couple hours after an exothermic run. When a sample was kept at room temperature for 3 days or longer, the next endotherm closely resembled the initial endotherm in area

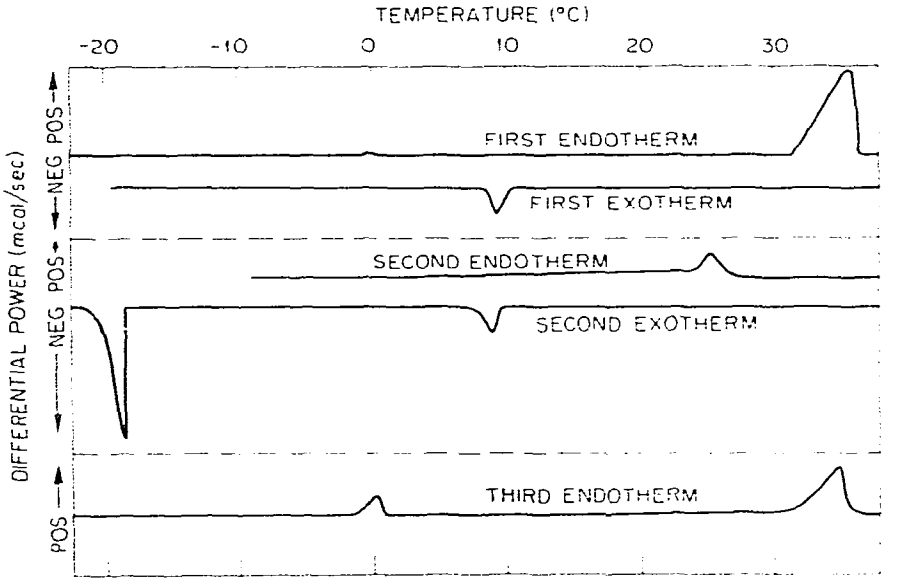

Fig. 2. Thermal spectra of 5.862 mg of $Na_2SO_4 \cdot 10\ H_2O$ in which a metastable phase, $Na_2SO_4 \cdot 7\ H_2O$ has formed. The exothermic deflections at 9°C represent the crystallization of $Na_2SO_4 \cdot 7\ H_2O$.

of the peak and also in the nearly complete disappearance of the transition near 0°C.

The spectrum of the second exotherm (again referring to Fig. 1) as well as subsequent exothermic scans were very similar to that obtained in the first exotherm. In some instances, the temperature of the peaks might be shifted by a few degrees and their areas somewhat different, but the dual-spiked profile remained the same.

For most of the samples of $Na_2SO_4 \cdot 10\ H_2O$, the thermal spectra just described reflected the more usual freeze—thaw behavior. However, in some cases a different profile was obtained (see Fig. 2). The initial endotherm, with a single well-defined peak at 35°C, was as expected. The first exotherm showed a peak at about 9°C, not of the usual spiked appearance of crystallization from a supercooled liquid. Instead, the peak was almost gaussian in shape; the area under the peak was equivalent to ~15 cal g^{-1} (of sample), or roughly 25% of the area recorded when fresh (or fully recovered $Na_2SO_4 \cdot 10\ H_2O$) is melted at 32°C. If the first exothermic scan is not carried to temperatures under −10°C, the next endotherm shows a peak beginning at 24°C instead of the peak at 35°C; this is shown as the "Second Endotherm" in Fig. 2. If the sample had been cooled low enough (−23 to −15°C) for a second peak to appear (note "Second Exotherm", Fig. 2) the next endotherm ("Third Endotherm", Fig. 2) would not show the peak at 25°C. This particular pattern of data occurs when a metastable phase, sodium sulfate heptahydrate ($Na_2SO_4 \cdot 7\ H_2O$), crystallizes from the liquid. Wetmore and LeRoy [5] note that solutions containing 33% Na_2SO_4 commonly form the crystalline heptahydrate when cooled below 17°C; once $Na_2SO_4 \cdot 10\ H_2O$ spontaneously crystallizes (see Fig. 2, at −19°C), the heptahydrate reverts to the more stable decahydrate by reacting with the solution.

For samples of $Na_2SO_4 \cdot 10\ H_2O$ with borax ($Na_2B_4O_7 \cdot 10\ H_2O$), differences in thermal spectra are shown by the dotted lines in Fig. 1. The high initial heat of fusion (55—57 cal g^{-1}) is not regained as a result of crystallization at 24°C; only about one-half is discharged at or near this temperature. On further cooling, another phase transformation occurred; on rapidly reheating to —1.5°C the absorbed enthalpy was equivalent to that released at —20°C. Continued reheating through the peritectic temperature shows a greatly diminished heat of fusion at 32°C; its value was dependent on the period of time the material had been kept at room temperature. The second exotherm routinely yielded results similar to those obtained from the first exotherm. The most notable difference caused by the borax is that the first transition on cooling appears at 24°C (dotted exotherms in Fig. 1), instead of at —2°C. The higher temperature indicates the effectiveness of borax as a precipitation catalyst. The relatively large extent of supercooling, 8°, would not have occurred with larger samples; the author [1] has shown that supercooling observed in DSC scans is greater than that observed in test-tube scale experiments. A less notable temperature difference occurs for the endothermic transition near 0°C. For samples with borax, one obtains a melting point of about —1.5°C, whereas for samples without borax the melting point is —1.1°C; in both cases the melting point is obtained from the leading edge of the endothermic peak. This small difference in melting points is consistent with information, reported from solubility measurements [2], which indicated that the ternary eutectic (for Glauber's salt, ice and borax) melts at a slightly lower temperature than the binary eutectic of Glauber's salt and ice. As with samples that did not contain borax, the energy discharged at the first exothermic transition was about the same, roughly 25—32 cal g^{-1}; borax did not lead to an increase in the amount of energy given off during crystallization. However, in greatly decreasing the extent of supercooling, the borax appeared to have prevented the precipitation of $Na_2SO_4 \cdot 7\ H_2O$; in no case were spectra of the type depicted in Fig. 2 observed for samples containing borax. On the basis of test-tube scale experiments, Hallett [6] also found that borax prevented the formation of the heptahydrate. The highest temperature reached by any of the samples was 42°C. In this instance, the heat of crystallization on cooling to about 24°C was ~25 cal g^{-1}, somewhat less than in other borax-containing samples for which lesser temperatures had been reached after melting. The time interval that a sample remained at or just over the melting temperature did not alter the general appearance of the next exotherm, nor did it seem to change the amount of heat discharged at 24°C. If the sample was kept at 32°C for a few seconds or for 18 h, the subsequent exotherm still exhibited the two thermal spikes. In the range of borax concentrations (2—9 wt.%) included with the $Na_2SO_4 \cdot 10\ H_2O$, neither the extent of supercooling nor the fraction of stored energy discharged at 24°C appeared to be a function of borax concentration.

In the discussion below, it will be suggested that the reaction between anhydrous Na_2SO_4 and a solution unsaturated with respect to Na_2SO_4 is essentially blocked by an enveloping layer of Glauber's salt. To determine if the formation of this blocking layer could be detected as a distinct phase transition, exotherms from 32.4°C to the transition at about 24°C were ob-

tained at the slowest cooling rates, 0.3125° min^{-1} and at instrument sensitivities where an enthalpy of transition as low as 50 μcal could be detected. No phase transitions were observed at these high instrument sensitivities. The negative results imply either a coating too thin to detect or else one that does not form prior to the transition at which Glauber's salt precipitates from solution.

Samples with borax and additional anhydrous Na_2SO_4 were studied to determine if additional Na_2SO_4 would promote equilibrium (peritectic) solidification of $Na_2SO_4 \cdot 10\ H_2O$. For molar ratios of $Na_2SO_4 : H_2O$ greater than 1 : 10, the phase diagram (see Fig. 3) shows no thermodynamically stable aqueous solution below the peritectic temperature. Samples of Glauber's salt with increments of 8.5, 12.2, or 36.1% anhydrous Na_2SO_4 were measured. For all three mixtures the results were nearly the same, and in no way did they appear to be dependent on the amount of Na_2SO_4 in excess of the 1 : 10 ratio of $Na_2SO_4 : H_2O$ in Glauber's salt. The initial heating absorbed 52—58 cal g^{-1}; the first and all other exotherms evolved 27—34 cal g^{-1} at 23—27°C. The second heating, if carried out within a few hours of the initial thermal cycle, absorbed about 30 cal g^{-1} at 32°C. After cooling to —25°C, the subsequent endotherm revealed a peak with a melting temperature of —1.5°C. Thus, the results were not different from those obtained without the incremental Na_2SO_4; additions of up to 36% Na_2SO_4 did not increase the fraction of stored energy that could be retrieved just below the peritectic temperature.

Several samples, all containing borax, were thermally cycled as many as 400 times between 19 and 36°C in the calorimeter. For these samples, the enthalpy of crystallization ranged between 26 and 32 cal g^{-1} $Na_2SO_4 \cdot$

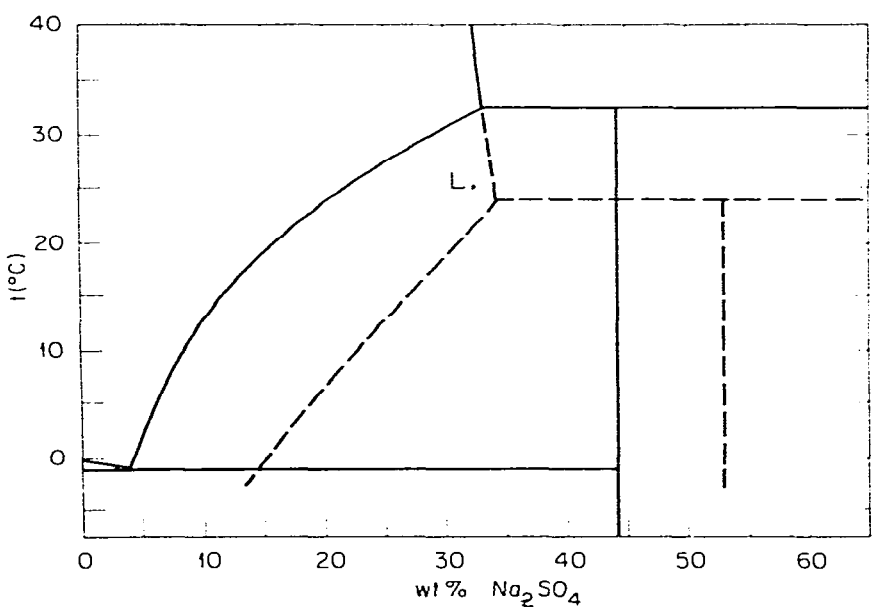

Fig. 3. Phase diagram of the $NaSO_4$—H_2O system constructed from data in ref. 2. Dashed lines refer to formation of $Na_2SO_4 \cdot 7\ H_2O$. At point L, solutions seeded with borax precipitate $Na_2SO_4 \cdot 10\ H_2O$ (see text).

10 H_2O. The enthalpy absorbed on melting near 32°C varied between 26 and 56 cal g^{-1}, lower values characteristic of short time periods between successive cycles. The initial endothermic measurement routinely yielded the highest enthalpy of transition. Similar to samples not containing borax, it appeared to take more than 3 days for a sample to recover its initial storage capacity. Details and further implications of these cycling studies as well as tabulated results of the extensive series of DSC measurements will be published elsewhere.

Before interpreting the results further it would be well to summarize certain experimental findings: (a) the enthalpy release, derived from the first and subsequent DSC exotherms, was roughly 30 cal g^{-1} $Na_2SO_4 \cdot 10\ H_2O$ in the sample, about one-half of the enthalpy absorbed on first melting; (b) continued cooling to temperatures less than —15°C led to the release, with supercooling, of additional energy, often as much as 15 cal g^{-1}; immediate reheating showed that this transition occurs just below —1°C, corresponding to a eutectic melting temperature for a mixture of ice and Glauber's salt (and also, where applicable, borax); (c) after the first thermal cycle, a relatively long period (at least 3 days) at room temperature was necessary to recover the full storage capacity of Glauber's salt; (d) anhydrous Na_2SO_4 added to Glauber's salt and borax did not alter the pattern of enthalpy absorption and release described by (a), (b) and (c); (e) borax, by greatly decreasing the extent of supercooling, seemed to prevent the formation of metastable $Na_2SO_4 \cdot 7\ H_2O$; (f) storage and discharge of energy at or near the phase transition temperature remained essentially constant at 30 cal g^{-1} over the first few (daily) thermal cycles; more rapid continuous cycling slightly decreased energy storage and discharge of $Na_2SO_4 \cdot 10\ H_2O$ to a level value of 26—27 cal g^{-1}.

It is clear from the foregoing that, upon cooling the mixture of solution and anhydrous Na_2SO_4 formed from Glauber's salt, stored energy was released by two processes which can be represented

concentrated soln. (~33 wt.% Na_2SO_4, peritectic soln. * compn.)

$$\rightarrow Na_2SO_4 \cdot 10\ H_2O + \text{less concentrated soln.} \quad (2)$$

$$\text{less concentrated soln.} + \text{anhyd } Na_2SO_4 \rightarrow Na_2SO_4 \cdot 10\ H_2O \quad (3)$$

Process (2), the crystallization of Glauber's salt from solution, is much faster than process (3). Because the integral heat of solution of Na_2SO_4 is so small, the heat of crystallization can be estimated from the negative of the heat of hydration of $Na_2SO_4 \cdot 10\ H_2O$ (—19.5 kcal $mole^{-1}$) [17]; by apportioning solution and Glauber's salt according to the lever rule applied to the phase diagram (at point L in Fig. 3) we obtain 27 cal for the enthalpy released from 1 g of material that was originally stoichiometric $Na_2SO_4 \cdot 10\ H_2O$. This calculated energy compares favorably with the 26—32 cal g^{-1} obtained from the exothermic phase transition for solutions that had supercooled to 24°C.

* The peritectic solution, by definition, would be saturated with respect to both $Na_2SO_4 \cdot 10H_2O$ and Na_2SO_4; the solution on the left of eqn. (2), at temperatures above 32.4°C, is no longer saturated with respect to Glauber's salt.

Besides the disparity between the initial heat of fusion (58 cal g^{-1}) and the observed heat of crystallization (about −26 cal g^{-1}), the slower reaction rate for process (3) can be qualitatively inferred from the significant transition observed at −1.5°C (−1.1°C without borax), the ice—Glauber's salt eutectic.

The sluggish reaction of Na_2SO_4 with the solution can be attributed to a layer of hydrate which encapsulates the anhydrate thereby limiting reaction with water to the slow process of solid-state diffusion. The DSC experiments, per se, provide no information regarding the nature of the coating around the anhydrous Na_2SO_4. However, an order of magnitude diffusion coefficient can be obtained: estimating that the radius or half-thickness of the Na_2SO_4 crystals is roughly 0.01 cm (probably a high estimate), and given that three days were necessary to convert all of the anhydrous Na_2SO_4 to Glauber's salt, we obtain a diffusion coefficient from the expression, $D = l^2/4\tau = (0.01)^2/(4 \times 3 \times 86,400) \sim 10^{-10}$ cm^2 sec^{-1}. This low value supports the idea of a crystalline diffusion barrier to reaction (3). Diffusion coefficients in aqueous liquids are about 10^{-5} cm^2 sec^{-1}, while those through an aqueous gel would be an order of magnitude lower, roughly 10^{-6} cm^2 sec^{-1}; for solids they are orders of magnitude smaller which appears to be the case in this instance.

The hypothesis of an encapsulating layer around the anhydrate was put forth by Biswas [8], suggesting that the layer was $Na_2SO_4 \cdot 10\ H_2O$ itself. But, if a layer of decahydrate forms on the anhydrate, what makes it stick so well? Further, why doesn't this decahydrate layer act to "seed" $Na_2SO_4 \cdot 10\ H_2O$ from solution? A possible mechanism that answers these questions is as follows. When a thin (perhaps monomolecular) layer forms on the anhydrate, heat is evolved (−19.5 kcal $mole^{-1}$ for ΔH of hydration of $Na_2SO_4 \cdot 10\ H_2O$) [7], raising the temperature of the crystal surface and the adjacent liquid. Two effects would follow from the local temperature increase: the hydrate layer would redissolve and more anhydrate would precipitate out under the driving force of the retrograde solubility. The low diffusion constant derived in this study suggests that only part of the decahydrate redissolves; indeed, one could imagine the first hydrate layer sandwiched by a layer of Na_2SO_4 which, in turn, forms another hydrate layer and so on. The key property in this mechanism is the negative temperature dependence of the solubility of Na_2SO_4.

The relevance of these measurements and their interpretation to the application of $Na_2SO_4 \cdot 10\ H_2O$ as a latent-heat-storage medium will be discussed elsewhere. Suffice it to say, that for static systems the energy (26—30 cal g^{-1} $Na_2SO_4 \cdot 10\ H_2O$) released by crystallization of the aqueous phase will be the only energy that can be reliably retrieved from storage. While this diminishes some of the potential of Glauber's salt as a storage material, it is of such low cost that it still remains a very attractive and viable candidate.

This discussion of $Na_2SO_4 \cdot 10\ H_2O$ closes with some remarks regarding its use as a thermometric standard. Glauber's salt is often proposed for this purpose on account of its relatively high heat of fusion and, perhaps because it melts somewhat beyond room temperature; when the scale of sample is about 100 g, the initially obtained temperature—time heating curve remains flat (at 32.38°C) for a long period of time. However, for sample sizes (1—50

mg) ordinarily used in DSC and in DTA equipment, it is much more difficult to obtain, on the initial heating, instrument conditions and sample purity sufficiently precise to produce sharp intersection between the baseline and the leading edge of the endothermic peak. Indeed, if the calibration obtained on first heating were not sufficiently accurate, it would be necessary to use a replicate sample or else wait several days before trying again with the same sample. In fact, the long-lived metastability of the aqueous solution that forms on melting, allows the Glauber's salt sample to be better applied as thermometric standard for —1.2°C, the eutectic temperature for mixtures of ice and $Na_2SO_4 \cdot 10\ H_2O$. Of course with the ice point being such a convenient thermometric standard, this eutectic would be of very limited usefulness.

$Na_4P_2O_7 \cdot 10\ H_2O$

The initial endothermic scan showed a very weak absorption peak near 0°C with an associated transition enthalpy of about 0.4 cal g^{-1} of sample. The eutectic temperature of ice and $Na_4P_2O_7 \cdot 10\ H_2O$ is —0.43°C [2]; the endothermic peak is, therefore, attributed to a slight excess of water in the sample. On continued heating a very strong absorption occurred at about 82°C. From the leading edge of this peak, a transition temperature of 79.5°C was obtained and this corresponds to the peritectic temperature [2] for this hydrate. The enthalpy of melting, derived from this peak, equalled 59 cal g^{-1}.

Upon immediately scanning downward, a transition appeared at 60°C; for other samples, this initial exothermic transition "spiked" in the range, 40—66°C. The enthalpy released by this transition varied between 26 and 35 cal g^{-1}; as Fig. 4 shows, the transition is supercooled. Further cooling revealed a second transition, also with the appearance of supercooling at

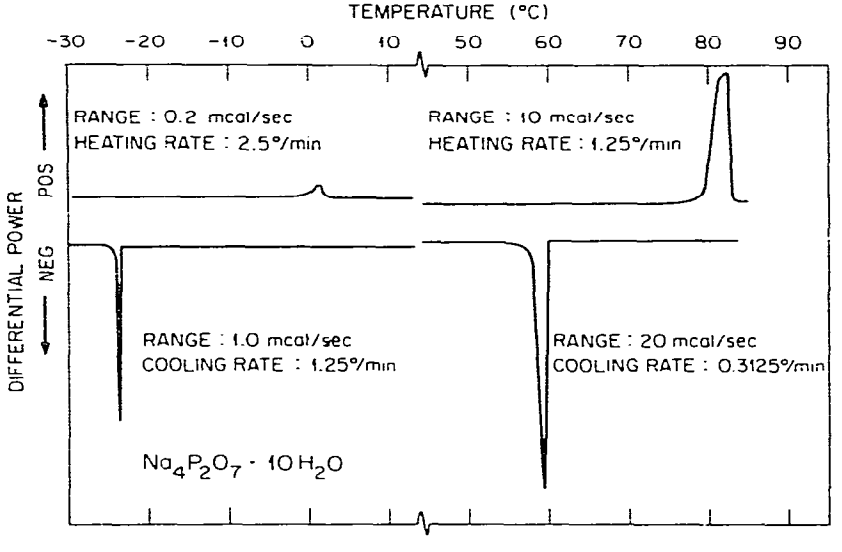

Fig. 4. DSC spectra of $Na_4P_2O_7 \cdot 10\ H_2O$, 7.775 mg. The exotherm was obtained immediately after the endothermic scan.

—24°C. Rapid reheating showed the transition near 0°C, greatly magnified; the enthalpy absorbed was about the same as that released at —24°C.

With the sample kept at 65°C for a time, subsequent heating scans showed the heat absorption at the peritectic to be 40—59 cal g^{-1}; lower values corresponded to the shorter periods at 65°C. In the case of a 6-mg sample held at 65°C for 40 min, the transition enthalpy at 79°C was 47 cal g^{-1}. A sample usually required overnight annealing to absorb the full enthalpy of fusion, 59 cal g^{-1}.

The test-tube experiments revealed that supercooling amounted to about 7°, considerably less than the 15 to 40° observed in DSC exotherms. At temperatures slightly greater than the melting point, the volume fraction of liquid appeared to be relatively small; the liquid was not visible as a distinct layer.

In several regards, the phase behavior of $Na_4P_2O_7 \cdot 10\ H_2O$ parallels that of $Na_2SO_4 \cdot 10\ H_2O$. Each of these decahydrates melts incongruently to form an anhydrate that exhibits retrograde solubility above the peritectic temperature. The DSC results showed other similarities. The first transition that occurs on cooling below the peritectic discharges less heat than can be absorbed at the peritectic; there is also an apparent stability of the aqueous solution as evidenced by the growth of a transition corresponding to the eutectic melting point of ice—$Na_4P_2O_7 \cdot 10\ H_2O$ mixtures.

As for $Na_2SO_4 \cdot 10\ H_2O$, the pattern of energy discharge observed for $Na_4P_2O_7 \cdot 10\ H_2O$ can be explained in terms of two processes: precipitation from the (supercooled) solution and formation of the decahydrate from anhydrate and solution; the former process occurs rapidly, the latter far more slowly.

From the temperature dependence of solubility of $Na_4P_2O_7 \cdot 10\ H_2O$, the enthalpy of solution can be estimated from the relation

$$\Delta H = -R \frac{\partial \ln N}{\partial (1/T)} \tag{4}$$

where N is the mole fraction of dissolved hydrate. Using the data tabulated in Linke's compilation [2], an enthalpy of solution of 17 kcal $mole^{-1}$ at 79°C is obtained. Applying this value to 0.635 g of solution that forms when 1 g of the decahydrate melts, yields 24 cal, somewhat less than the 26—35 cal g^{-1} of sample observed as the enthalpy of crystallization. The higher observed value may indicate that some reaction between anhydrate and solution seems to occur simultaneously with the crystallization of hydrate from solution.

Another apparent difference in the behavior of this hydrate as compared to Glauber's salt arises from the higher temperature of the peritectic transition. The higher temperature leads to higher diffusion rates and this probably accounts for the more rapid recovery of the full energy-storage capacity of $Na_4P_2O_7 \cdot 10\ H_2O$. The higher temperature also leads to a lower viscosity for the solution which may account for the milder supercooling observed both in the DSC and in the test-tube experiments.

$Mg(NO_3)_2 \cdot 6\ H_2O$

Endothermic scans showed two peaks, a weak one at about 75°C and a much stronger one, peaking at about 92°C. From the leading edge of the larger peak a transition temperature of 90°C was obtained in excellent agreement with the melting point of 89.9°C given in Circular 500 [7]; the area of this peak yielded a ΔH of fusion of 36.2 cal g^{-1}. The ΔH of transition calculated from the lesser peak was 2.9 cal g^{-1}; from the leading edge, the transition temperature of 73°C was derived.

Exothermic scans generally yielded a profile with two peaks, but as Fig. 5 shows, the smaller peak is not fully resolved and the crystallization peak reveals the effect of supercooling; in this case, the liquid supercooled about 15° before crystallizing. Exotherms of other samples occasionally showed the solid transition peak as a supercooled spike. The solid-state transition was usually detected exothermically at 68°C.

Thermal cycling of $Mg(NO_3)_2 \cdot 6\ H_2O$ generally showed that ΔH of crystallization was equal to ΔH of fusion. For runs where the area due to the solid transition could not be resolved from exothermic scans, the area of the combined exothermic peaks was the same as the sum of the two areas measured in the subsequent endotherm.

The only previously reported [9] calorimetric determination gives a value of 38.2 cal g^{-1} for ΔH of fusion. However, this measurement may also have included the enthalpy of transition in the determination. Thus, the value of 36 cal g^{-1} derived in this work is probably more accurate.

The enthalpy of the solid-state transition (2.9 cal g^{-1}) has not previously been reported. The existence of this transition was first reported by Pouillen

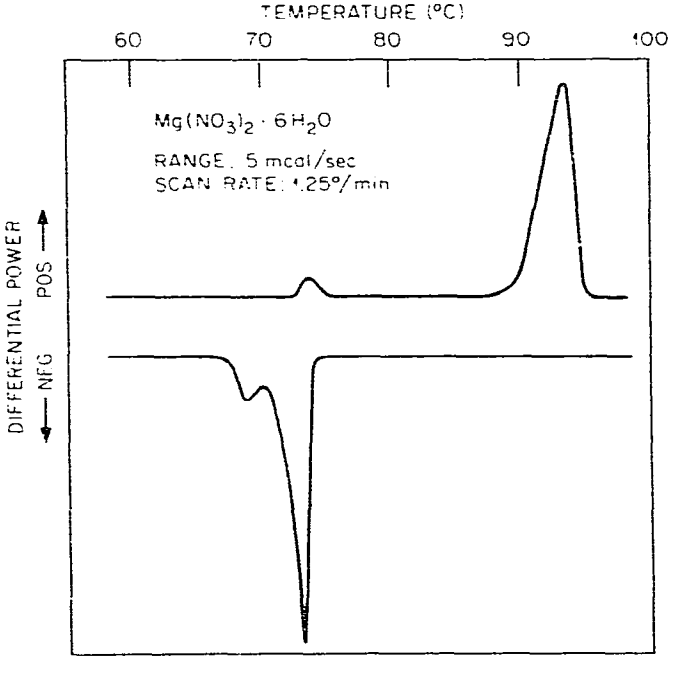

Fig. 5. Endotherm and exotherm of $Mg(NO_3)_2 \cdot 6\ H_2O$, 3.767 mg.

[10] from DTA and dilatometry, the latter indicating a 0.4% volume contraction upon heating through the transition.

$MgCl_2 \cdot 6\ H_2O$

Melting and freezing were recorded as single peaks (see Fig. 6). The melting point as derived from the leading edge of the endothermic peak was 116°C; however, a sharp melting point was not obtained, probably because of the slight excess of water in the sample material. The onset of crystallization at 90—97°C was very easily discerned because of supercooling.

The highest value obtained for the heat of fusion was 39.9 cal g^{-1}, in good agreement with the 40.3 cal g^{-1} given in NBS Circular 500 [7]. Other values for ΔH of fusion obtained by DSC ranged downward to 32 cal g^{-1}. The magnitude of the enthalpy of crystallization usually matched the enthalpy of fusion obtained from the preceding endotherm, provided the cooling rate was 1.25° min^{-1} or less. At cooling rates of 2.5—10° min^{-1}, ΔH of crystallization appeared to be 5 to 20% less in magnitude than the ΔH of fusion.

The test-tube experiments yielded a different pattern of results. Melting was observed to occur over a range of temperatures; some liquid was visible at 117°C and the sample completely liquefied at 120°C. On cooling of the melt, virtually no supercooling took place; freezing occurred at 117°C from a clear liquid. No solid hydrolysis products [e.g., MgOHCl, $Mg(OH)_2$] were visible in the melt. The lack of hydrolysis was confirmed by checking the vapor space for HCl with pH paper once the sample had been quenched.

The phase diagram of the $MgCl_2$—H_2O system constructed from the solubility data [2] indicates that complete melting of the hexahydrate occurs in two steps: first at 116.7°C, the formation of a relatively small amount of

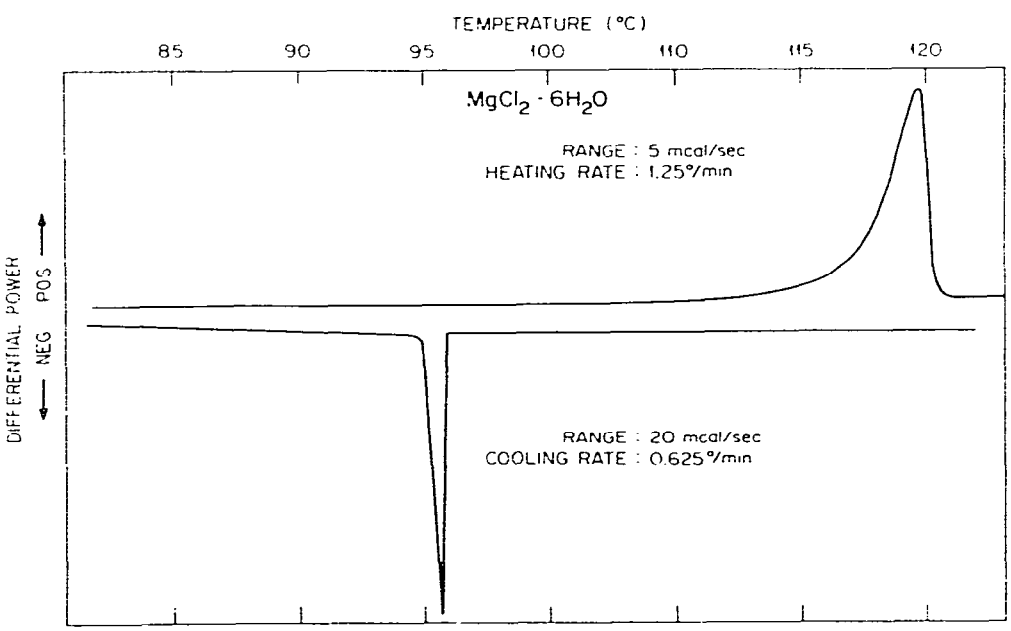

Fig. 6. Endotherm and exotherm of $MgCl_2 \cdot 6\ H_2O$, 3.352 mg.

tetrahydrate in equilibrium with a relatively large amount of solution; second, dissolution of the tetrahydrate over the range, 116.7—120°C. The test-tube experiments qualitatively confirmed the two-step melting but the DSC endotherms did not. Freezing in both type of experiments appeared to be congruent, i.e., the melt solidified to the hexahydrate without going through the tetrahydrate step.

$CuSO_4 \cdot 5\ H_2O$

The heat of fusion obtained from slow heating scans was 32 cal g^{-1} and the melting point was found to be about 96°C.

Cooling scans showed only one transition occurring somewhere in the range 30—60°C. The ΔH of transition, evaluated exothermically, varied between 12—19 cal g^{-1}; subsequent endotherms yielded 30—32 cal g^{-1}. Cooling of samples down to —50°C and subsequent heating did not reveal the ice—$CuSO_4 \cdot 5\ H_2O$ eutectic temperature which is reported to occur at —1.5°C [3].

The test-tube experiments indicated that the solution supercooled to 82°C before freezing. As with $Na_4P_2O_7 \cdot 10\ H_2O$, the volume fraction occupied by the liquid phase just above the melting point appeared to be relatively small.

Neither the DSC results nor the test-tube experiments permit an unequivocal statement regarding the presence or absence of barriers to solidification.

$Na_2B_4O_7 \cdot 10\ H_2O$

Initial melting of a sample annealed overnight at 45°C yielded an enthalpy of transition of 33 cal g^{-1}. The leading-edge melting point was 60.5—61°C. The endothermic transition was usually recorded as a double peak (see Fig. 7).

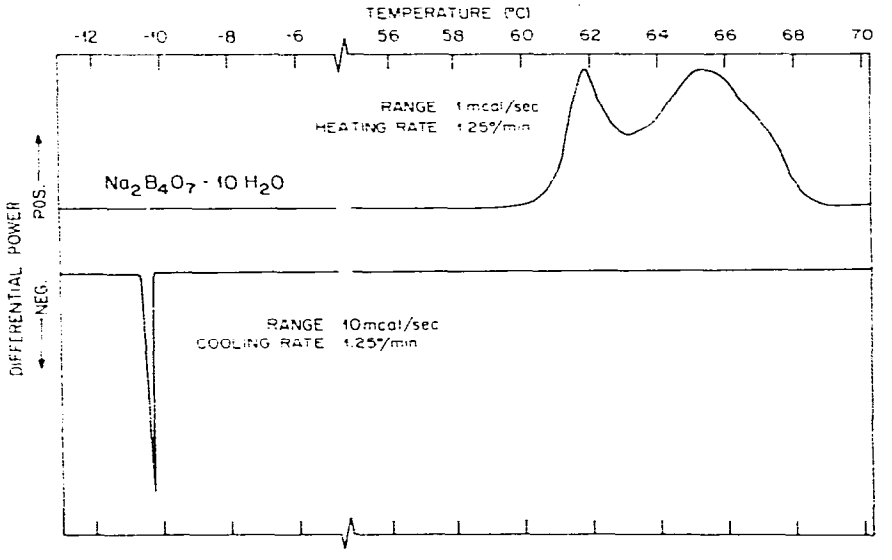

Fig. 7. Endotherm and exotherm of $Na_4B_2O_7 \cdot 10\ H_2O$, 2.814 mg.

Exothermic runs always revealed a (very extensively supercooled) transition at −10 to −15°C, at which 10–15 cal g^{-1} was released. Heating scans taken soon after showed a transition at −1°C; the eutectic temperature for ice–borax mixtures is −0.43°C [2]. The absence of an exothermic transition between 60 and −10°C probably signifies that the crystallization of borax from solution may be prevented by supercooling. It is very improbable that the thermal resistance of the pentahydrate or the tetrahydrate (formed on melting) was sufficiently great to prevent detection of the crystallization.

The phase transition obtained endothermically is believed to form the metastable pentahydrate ($Na_2B_4O_7 \cdot 5\ H_2O$) rather than $Na_2B_4O_7 \cdot 4\ H_2O$; the derived melting point was 60.5–61°C instead of 58.5°C, the peritectic temperature at which the tetrahydrate is in equilibrium with borax. Blasdale and Slansky [11] reported that upon heating borax at a uniform rate, the temperature–time curve yielded 60.8°C for the decahydrate–pentahydrate transition point.

The transformation of borax to the pentahydrate can also be rationalized from the magnitude observed for the heat of fusion. We note from Table 1 that the transformations can be written

1 mole borax → 0.9 mole tetrahydrate + 0.1 mole dilute soln.

and

1 mole borax → 0.9 mole pentahydrate + 0.1 mole of a somewhat less dilute soln.

Because of the low solubility of $Na_2B_4O_7$, these reactions, are to a reasonable approximation, almost equivalent to dehydration reactions

$$Na_2B_4O_7 \cdot 10\ H_2O \rightarrow Na_2B_4O_7 \cdot 4\ H_2O + 6\ H_2O(l) \quad (5)$$

$$Na_2B_4O_7 \cdot 10\ H_2O \rightarrow Na_2B_4O_7 \cdot 5\ H_2O + 5\ H_2O(l) \quad (6)$$

ΔH_{298} (rcn. 5) = 14.4 kcal $mole^{-1}$ [7]. ΔH_{298} (rcn. 6) = 12.0 kcal $mole^{-1}$. Using $\Delta C_p \sim 9$ cal deg^{-1} per mole of H_2O for these reactions (as suggested by Phillipson and Finlay [12]), raises enthalpies at 60°C by about 0.2 kcal $mole^{-1}$; thus ΔH_{333} (rcn. 5) = 14.6 kcal $mole^{-1}$ = 38.3 cal g^{-1}; ΔH_{333} (rcn. 6) = 12.2 kcal $mole^{-1}$ = 32 cal g^{-1}. The observed heat of fusion, 33 cal g^{-1}, is clearly much closer to ΔH_{333} for dehydration to the pentahydrate.

In test-tube experiments when borax was heated to 70°C, about 10° above the melting point, little or no liquid was visible. Slow cooling to 35°C showed no break in the temperature–time curve; either crystallization of the small amount of liquid was not detected by the thermocouple, or else extensive supercooling, as observed in the DSC, also occurs in the far larger test-tube samples. Obviously borax would be a very inferior material for latent-heat storage.

ACKNOWLEDGEMENTS

This research was supported by the Division of Energy Storage Systems, U.S. Department of Energy under contract with Union Carbide Corporation (Contract W-7405-eng-26). The author whishes to thank Mr. Tom Gayle, ORNL, for designing and assembling the electronic integrator used in conjunction with the DSC measurements. I am also grateful to Dr. John Ricci, Professor Emeritus, NYU, and to Dr. Jerry Braunstein, ORNL, for their very helpful discussions.

REFERENCES

1 S. Cantor, Thermochim. Acta, 26 (1978) 38.
2 W.F. Linke and A. Seidell, Solubilities, American Chemical Society, Washington, D.C., 4th edn., Vol. I, 1958; Vol II, 1965.
3 J. D'Ans, H.E. Freund and N.H. Woelk, in Landolt-Börnstein Zahlenwerte und Funktionen, Band 2, Teil 2b, 1962, pp. 3-29, 3-39, 3-167.
4 G. Brodale and W.F. Giauque, J.Am. Chem. Soc., 80 (1958) 2042.
5 F.E.W. Wetmore and D.J. LeRoy, Principles of Phase Equilibria, McGraw-Hill, New York, 1951, pp. 31–53.
6 J. Hallett, personal communication, University of Nevada, Desert Research Institute, Reno, Nev., 1977.
7 F.D. Rossini, D.D. Wagman, W.H. Evans, S.Levine and I. Jaffe, Selected Values of Chemical Thermodynamic Properties, National Bureau of Standards Circular 500, U.S. Govt. Printing Office, Washington, D.C., 1952.
8 D.R. Biswas, Sol. Energy, 19 (1977) 99.
9 E.H. Riesenfeld and C. Milchsack, Z. Anorg Chem., 85 (1914) 421.
10 P. Pouillen, C.R. Acad. Sci., 250 (1960) 3318.
11 W.C. Blasdale and C.M. Slansky, J. Am. Chem. Soc., 61 (1939) 918.
12 A. Phillipson and G.R. Finlay, Can. J. Chem., 54 (1976) 3163.